Using street based metrics to characterize urban typologies

T. Hermosilla [ab], J. Palomar [ab], A. Balaguer-Beser [ac], J. Balsa-Barreiro [d], L.A. Ruiz [ab]

[a] Geo-Environmental Cartography and Remote Sensing Group, Universitat Politècnica de València, Camino de Vera, s/n 46022, Valencia, Spain

[b] Department of Cartographic Engineering, Geodesy and Photogrammetry, Universitat Politècnica de València, Camino de Vera, s/n 46022, Valencia, Spain

[c] Department of Applied Mathematics, Universitat Politècnica de València, Camino de Vera, s/n 46022, Valencia, Spain

[d] Department of Mathematical Methods and Representation, Universidade da Coruña, Campus de Elviña s/n, 15071A Coruña, Spain

Corresponding author: Txomin Hermosilla
e-mail: txohergo@topo.upv.es
Postal address:
Departamento de Ingeniería Cartográfica, Geodesia y Fotogrametría
Camino de Vera, s/n. 46022 Valencia. SPAIN
Telephone: +34 96387000 Ext 75576
Fax Number: +34 963877559.

Abstract

The urban spatial structure reflexes the local particularities produced during the historical development of a city. Currently high spatial resolution imagery and LiDAR data are used to derive numerical attributes to characterize the intra-urban structure and morphology. The urban-block boundaries have been frequently used to define the units to extract metrics from the remotely sensed data. In this paper, we propose to complement those metrics with a set of descriptors of the streets surrounding the urban blocks that numerically characterize the geometry, presence of vegetation, and relationship with buildings. To carry out this purpose we also introduce a methodology to define the street area related with an urban block from which derive the urban metrics referred to the street. The assessment of these metrics is fulfilled using one-way ANOVA procedure and decision trees classifier. These results reveal that street metrics, and particularly those describing the street geometry, are suitable to enhance the

discrimination of complex urban typologies. Thus, the overall classification accuracy increases from 72.7% to 81.1% when adding the street descriptors. The results of this study demonstrate the usefulness of the metrics describing the street properties to complement the information derived from the urban blocks and to improve the characterization of urban areas.

Highlights

We propose a set of urban metrics to describe the streets with remotely sensed data

A methodology to relate the street space to urban blocks is defined

Results show that street metrics are useful to improve the characterization of cities

Keywords:

Urban morphology; urban metrics; remote sensing; high-resolution imagery; LiDAR

1. Introduction

Landscape metrics were defined by McGarigal and Marks (1995) as measurements that enable to numerically quantify and summarize the spatial patterns of the land-use/land-cover (LULC) classes of a geographic area. The urban spatial structure reflects the processes that occur during the historical development of a city, so urban districts constructed in different time periods show significant differences in building density and structures (Anas et al., 1989; Yu et al., 2010). The geometry of open spaces and built-up areas composing a city and their topological relationships determine the appearance of urban environments, and display local particularities related to a spatial identity (Laskari et al., 2008). Therefore, the various urban structural typologies can be depicted through metric attributes quantifying characteristics such as shape, land cover composition, spatial arrangement, or contextual relationships. The use of those urban metrics has become a trend in a wide range of studies and applications (Ji et al., 2006), e.g., environmental monitoring (Robinson, 2006; Edussuriya et al., 2011), energy efficiency assessment (Neidhart and Sester 2006; Geiß et al., 2011; Kellett et al., 2013; Tooke and Coops, 2013), socio-economic analysis (Patino and Duque, 2012; Tompalski and Wężyk, 2012; Gong et al., 2013), hydrological studies (Canters et al., 2007), or, with significant importance, in LULC mapping and change detection (Furberg and Ban 2008; Novack et al., 2010; Malinverni, 2011; Hermosilla et al., 2012a; Hermosilla et al., 2012b).

Remote sensing data have a relevant role to provide automatic and massive structural descriptions of urban areas (Puissant et al., 2012). High spatial-resolution multi-spectral information acquired from satellites or airborne sensors enable a detailed characterization of urban areas. In addition, airborne LiDAR (Light Detection And Ranging) systems facilitate a three-dimensional description of the landscape providing point clouds representing the height distribution of the observed terrain and the aboveground elements. When working with remotely sensed data, urban characterization is commonly undertaken applying two stage approximation methods (Bauer and Steinnocher, 2001). Initially, the principal LULC or the basic elements, such as buildings or vegetation, are identified. Then this information is analyzed in a spatial context to define urban metrics describing aspects such as the geometry, dimensions, or the area covered by buildings, vegetation, or other construction materials. In this analysis of urban morphology, remote sensing may take advantage of the physical explicitness represented by urban blocks, since roads and/or cadastral maps incontrovertibly delimit them (Yoshida and Omae, 2005). An urban block is defined as the group of private or public buildings and open space composing an island surrounded by public roads or streets (Gil et al., 2012). Using urban blocks would facilitate combining multiple datasets to analyze and characterize urban areas, and also integrating the information derived from remotely sensed data into GIS (Geographic Information Systems) (Gamba et al., 2005). As a consequence, numerous authors have employed urban blocks – or occasionally parcels – to define units from which extract metrics from high-spatial resolution images (Zhan et al., 2000; Kressler et al, 2001; Bauer and Steinnocher, 2001; Wijnant and Steenberghen, 2004; Pan et al., 2008; Wu et al., 2009; Novack et al., 2010; Vanderhaegen and Canters, 2010; Huck et al., 2011). These metrics are complemented with height information and volumetric descriptor sets whether three-dimensional information is available (Yoshida and Omae, 2005; Wu et al., 2009; Yu et al., 2010; Hermosilla et al., 2012a; Heiden et al., 2012; Taubenböck et al., 2013).

In addition to bounding the blocks, urban-block cartography enables to delimitate as its complementary area the public streets. Street properties such as shape and geometry, or the presence of diverse vegetation are also factors determining the appearance of the urban space (Lillebye, 1996). Hence, the characterization of the streets surrounding an urban-block may provide a contextual frame to highlight the differences between urban structural typologies. However, the discriminative potential of attributes based on the streets have been barely explored in the literature, which have been mainly focused in the geometrical description of the streets. In this sense, Loüw and Sithole (2011) characterized urban blocks with a set of street-based descriptors such as street width or building-street distances; Gil et al. (2012) used properties such as dimensions, orientation, accessibility, or connectivity to describe the streets. Both works considered the streets as linear features. We propose to complete and complement the geometrical description of the streets with information computed from remote sensing data. This would enable to describe deeper the urban landscape using additional characteristics derived from the streets – considering these as polygon features –, such as the presence and distribution of vegetation, or the relationships of street geometry with the surrounded buildings.

This requires an initial process to partition the street space and to find its dependencies to the urban-blocks.

This paper aims (i) to propose a methodology for partitioning the public street space and relate it to each urban block; (ii) to define a set of urban metrics based on the streets surrounding the urban blocks; and (iii) to perform a comprehensive statistical analysis of the usefulness of the proposed metrics. This is done by studying the complementariness of the street metrics to urban blocks metrics for discriminating among several urban typologies in the metropolitan area of Valencia (Spain). The paper is structured as follows. In Section 2 the study area, the high-spatial resolution images and the LiDAR data are described. Section 3 describes the methodology followed: definition of urban typologies within the studied area, procedure to derive the street area related to the urban block, the compilation of the urban-block based metrics and the definition of street-based descriptors, and finally the methodology followed to assess the metrics. The statistics and classification results are presented and discussed in Section 4. Section 5 provides the conclusions.

2. Study area, data and preprocessing

We performed this study in the city of Valencia, the third most populated city in Spain. The demolition of the medieval wall and the subsequent processes of annexation of nearby villages as own neighbourhoods in the second half of the nineteenth century leaded a process of urban expansion relatively concentric to the historical city. The strong industrialization process experienced in the 1950s-1960s and the rapid increase of population produced by the urban exodus disturbed the planned urban model. The subsequent processes to connect the city to the sea directed the urban sprawl eastwards, producing an absorption of satellite historical settlements within the new city (Balsa-Barreiro and Lois-González, 2009).

Remotely sensed data – high spatial-resolution imagery and LiDAR – were acquired in the frame of the Spanish National Plan of Aerial Orthophotography (PNOA). The images were collected in August 2008, with 0.5 m/pixel spatial resolution, 8 bits radiometric resolution, and four spectral bands: infrared, red, green, and blue. The images are distributed orthorectified and georreferenced, panchromatic and multispectral bands fused, and with mosaicking and radiometric adjustments applied. LiDAR data were collected in September 2009 using a RIEGL LMS-Q680 laser scanner with a scan frequency of 46 Hz, 70 kHz of pulse repetition rate and a scanning angle of 60º. The mean flying height was 1,300 meters, a nominal density of 0.5 points/m^2 and an average density value of 0.7 points/m^2. A normalized digital surface model (nDSM), i.e., the difference between the digital surface model (DSM) and the digital terrain model (DTM), representing the physical heights of the elements present over the terrain, was generated from LiDAR data. The DTM was computed using an algorithm that iteratively selects minimum elevation points and eliminates points belonging to any aboveground elements, such as vegetation or buildings (Estornell et al., 2011).

Urban block boundaries are provided in vector-format cadastral cartography with a scale of 1:1,000. These maps are produced by the Spanish General Directorate for Cadastre (Dirección General de Catastro).

Numerous urban metrics defined are based on the building and vegetation covers, which were obtained using an automatic building detection technique consisting of applying a multiple-threshold based approach over the normalized difference vegetation index (NDVI) image and the nDSM. This methodology is fully described and assessed in Hermosilla et al. (2011).

3. Methodology

3.1. Urban typologies

We defined eight urban typologies representing different historical periods of edification and urban planning of Valencia, and selected samples based on the visual analysis of the urban structure over the high-spatial resolution images. The urban typologies defined are:

- Main historical town (*historical1*) which constitutes the historical core of the city. Their irregular geometrical shape characterizes blocks, which are surrounded by very narrow streets and few green zones. The buildings show a variety on their heights (Figure 1.a).
- Secondary historical town (*historical2*): it refers to minor historical settlements integrated now within the city. Urban-blocks are spatially arranged with varied regularity, and the buildings are usually lower than in the main historical town (Figure 1.b).
- Late XIX century expansion (*rXIX*) – denoted ensanche in Spanish – developed in regular grid plan, with significant mid-block open spaces. Although initially the height of the buildings was related to the adjacent streets, most these requirements were later modified (Figure 1.c).
- Residential areas built in 1950 and 1960 decades (*r1950-60*): these neighbourhoods were developed with hurry in order to shelter the displaced population due to the rural flight. This typology is composed by average-height buildings placed in barely regular urban-blocks, which are usually delimited by narrow streets (Figure 1.d).
- Residential areas from 1970 and 1980 decades (*r1970-80*): composed by especially tall apartment towers and open public spaces like plazas and gardens (Figure 1.e).

- Residential areas built-up during 2000 decade (*r2000*) present also high buildings and abundance of gardens – both within public and private locations –, in urban-blocks bounded by wide avenues (Figure 1.f).
- Single-family suburban areas (*suburban*): groups of detached and semi-detached individual buildings, often surrounded by vegetation and located at certain distance of the core of the city (Figure 1.g).
- Industrial areas (*industrial*): planed zones populated with buildings and structures for manufacturing, transforming, repairing, storing, and distributing goods. Constructions are usually extensive and arranged to the street network (Figure 1.h).

3.2. Urban block related street area (UBRSA) definition

We state public street as those areas in the city that are enclosed by no urban block. The urban-block related street area (UBRSA) polygon is the specific public street surrounding each urban block, and this is understood as the street area related by an urban block. We developed a methodology to define spatially the UBRSA polygons by triangulating the public street and detecting the intersections of the streets. As result, the street is divided in street segments, which are afterwards merged producing the UBRSA polygons related to each urban-block, from which the metrics are derived.

First, the contour of urban-blocks is simplified using the point remove algorithm, an enhanced version of the Douglas-Peucker algorithm (Douglas and Peucker, 1973), in order to remove unrelevant details and increase processing efficiency (Figure 2.a). Next, the public street polygon is extracted as the complementary area of urban block polygons (Figure 2.b).

The street polygon is then partitioned in street segments delimited by the street crossing boundaries. This process is based on the triangulation of the public street polygon, which is a computational geometry process where for a set of points in a plane (the street polygon vertices) produces a triangulated irregular network (TIN). These triangles represents a surface as a set of non-overlapping contiguous triangular facets with irregular size and shape (Fowler and Little, 1979). That way, every triangle of the TIN within the street polygon (Figure 2.c) is analysed to detect the street crossings. Thus, a triangle belongs to a street intersection area if none of its edges is adjacent to an urban block. Once these triangles are detected, street crossing boundaries are determined by drawing a line from its centroid to each of its vertices (Figure 2.d). If several adjacent triangles are contained in a street intersection, the centroid computed is the one referred to the polygon composed by all these triangles. Figure 3 shows examples of how street crossing boundaries are defined for one (Figure 3.a), two (Figure 3.b), or three (Figure 3.c) triangles contained within a street intersection. Next, the triangles are merged keeping the street crossing boundaries (Figure 2.e) and producing, as a result, the division of the street polygon in several street segments (Figure 2.f).

The last step is the creation of the UBRSA polygons. Thus, the UBRSA polygon of an urban-block is produced by merging every adjacent street segment to that block. Since a street segment is likely adjacent to several urban-blocks, most UBRSA polygons of neighbouring blocks will overlap among them, as shown in Figure 4.

3.3. Descriptive urban metrics

We defined two groups of urban metrics: urban-block-based metrics, and street-based metrics derived from the UBRSA polygons. To characterize the urban-blocks three kinds of metrics were used: (i) descriptors of the shape and geometrical properties of urban-block polygons, (ii) geometric and volumetric attributes regarding buildings, and (iii) features describing vegetation patches. Most of these urban-block metrics, or variations thereof, have been repeatedly used in urban characterization (Boffet and Rocca-Serra, 2001; Yoshida and Omae, 2005; Neidhart and Sester, 2006; Laskari et al., 2008; Goodwin et al., 2009; Van de Voorde et al., 2009; Lu et al., 2010; Yu et al., 2010; Tooke et al., 2011; Heiden et al., 2012; Hermosilla et al., 2012a; Peeters and Etzion, 2012, Berger et al., 2013; González-Aguilera et al., 2013). The geometry of the urban-block polygons is described with the area and perimeter, meanwhile the contour complexity is numerically quantified using the shape factors: compactness, shape index, and fractal dimension. Compactness (or circularity) measures the degree to which the shape is close to a circle (Bogaert et al., 2000). Shape index estimates how similar to a square a shape is. Fractal dimension provides a numerical characterization of fractal patterns by computing their complexity as a ratio of the change in detail to the change in scale (Krummel et al., 1987; McGarigal and Marks, 1995). Buildings are described in terms number, area, height, and volume. The built-up area is characterized by means of the building coverage area (*BCA*) and the building covered ratio (*BCR*). *BCR* is obtained by normalizing the *BCA* by the area of the urban block, expressing the result as percentage. The number of buildings within the urban block (N_B) is also computed. The height of the buildings is characterized using the mean ($\overline{BH}$), maximum (*maxBH*), and standard deviation (*sdBH*) values obtained from the nDSM. Using this model, the volumetric properties of the buildings are also derived. In addition to the built-up volume ($Volume_B$), the mean built-up volume per building ($\overline{Volume_B}$), and the built-up volume normalized by the urban-block area ($nVolume_B$) are computed. Analogously, vegetation metrics computed are vegetation covered area (*VCA*), vegetation covered ratio (*VCR*), vegetation volume, and vegetation volume normalized by urban-block area. Table 1 compiles the equations to compute the urban-block based metrics.

The street-based urban metrics characterize the UBRSA in terms of four aspects: geometry, neighbouring block connectivity, presence of vegetation, and relationship with the urban-block buildings. The geometry of the streets is quantified by means of the area ($Area_{UBRSA}$) and descriptors of the width of the street segments composing the UBRSA of an urban block. The width of each street segment is computed by initially enclosing an oriented bounding rectangle. The major axe orientation is then used as guide to draw perpendicular transects separated apart one metre, as it is shown in Figure 5.a. The median width of all transects is assigned as the specific width of the street segment. Finally, the mean ($\overline{SW}$), standard deviation ($sdSW$), minimum ($minSW$), and maximum ($maxSW$) of the width of the adjacent street segments are computed (see Figure 5.b). The number of neighbouring urban blocks (NN_{UB}) of each UBRSA polygon provides the degree of neighbouring block connectivity. The vegetation metrics characterizing the streets are vegetation covered area (VCA_{UBRSA}), vegetation covered ratio (VCR_{UBRSA}), vegetation volume ($Volume_{VUBRSA}$), and vegetation volume normalized by UBRSA area ($nVolume_{VUBRSA}$). The last group of street-based metrics aims to relate the structure of the buildings of an urban block to the geometry of the surrounding streets, and to exploit the dependency relationships among them. The metrics computed are the ratio between the BCA of a block and the area of its UBRSA ($Ratio_{Area}$), and the ratio between the built-up volume within a block normalized by the UBRSA area ($Ratio_{Volume}$). Table 2 summarizes the equations to compute the street based metrics.

3.4. Assessment of the metrics

Initially, we studied the metrics independently by applying the one-way ANOVA procedure to estimate the ability of each urban metric to describe the differences among the eight urban typologies. The F-test in the ANOVA table, which is defined as the ratio of the between-group variance estimate to the within-group variance estimate, evaluate whether there are any significant differences amongst the means. In addition, the Fisher's least significant difference (LSD) procedure (Milliken and Johnson 1992) is also employed to determine which means are significantly different from which others in such a way that if two means are the same then their intervals will overlap 95% of the time. To avoid the effects of outliers, we also have applied the Kruskal-Wallis test to compare median instead of mean values.

To evaluate the performance of the proposed street urban metrics, we performed two classifications: one considering the urban-block metrics, and other combining these with the street metrics. We applied the C5.0 algorithm using See5.0 software (Quinlan, 1993). Preceding the creation of the rules for each classification, an initial selection of the metrics was performed in order to reduce number of descriptive attributes to be used into the classifier, in addition to estimate their impact in the classification. This process, denoted winnow (Littlestone, 1988), numerically estimates the importance of the descriptive attributes for the particular classification problem analyzed, enabling to choose the useful metrics among unhelpful ones. The selected attributes are then ranked by importance, numerically showing for each attribute the percentage increase in error rate if that attribute is excluded from the classification.

The C5.0 algorithm defines decision trees were constructed based on training samples. A decision-tree is defined as a set of conditions organized in a hierarchical structure in such a way that the class assigned to an object is determined following the conditions that are fulfilled from the initial dataset to any of the assigned classes. A two-step pruning process was applied to the decision trees to reach a better predictive accuracy by reducing the over-fitting. Initially, the degree to which the initial tree fits the training data was constrained by fixing a minimum of five training cases that each node must follow. Later, the parts of the decision trees predicted to have a relatively high error rate were removed. This was first applied to every sub-tree to decide if it should be replaced by a leaf or sub-branch or not, and then a global stage considers the performance of the tree as a whole (Murthy, 1998).

Decision trees were applied in combination with the boosting technique, which allows for the increase of the classifier accuracy by constructing multiple decision trees (Freund et al., 1999). This technique relies on assigning weights to the training samples, so the greater the weight of a sample, then the greater its influence on the classifier. After each tree construction, weights are adjusted to show the model performance. Samples erroneously classified maintain their assigned weights, whereas correctly classified samples reduce their weights. As result, the model obtained in the subsequent iteration provides more relevance to the earlier incorrectly classified samples. We used ten iterations to define the rules. After the construction of the decision tree set, the class assigned to an object considers the estimated error produced in the construction of each tree, being the weight assigned to a tree inversely proportional to the estimated error. The summation of the weights of the trees predicting the same class is then computed, and the class with the highest value is finally assigned.

The accuracy of the classification models was assessed using leave-one-out cross-validation technique (Fukunaga, 1990). Both classifications were evaluated by analyzing the confusion matrix (Congalton, 1991), which relates the class assigned to each test sample with its reference class. We computed the overall accuracies of the classifications, and for each class, producer's and user's accuracies, which respectively estimate the mission and commission errors.

4. Results and discussion

The one-way ANOVA results show that the p-value of the F-test for all metrics is lower than 0.05, meaning that there are statistically significant differences between the mean values of the urban typologies with 95% confidence level. In addition, the results of the Kruskal-Wallis test show significant differences for all variables among the medians of the eight urban typologies with 95% confidence. Table 3 identifies with letters (A, B, C, etc.) the resulting homogeneous groups using the Fisher's LSD multiple comparison procedure to discriminate among the means. Figure 6 visually shows examples of buildings and vegetation occupation and height distribution for the various urban typologies defined. Finally, Figure 7 and Figure 8 illustrate the relationship of the urban typologies with the urban block metrics and the street metrics, respectively, using box-and-whisker plots showing median, interquartile range (IQ), and extreme values. Circles indicate atypical outliers (values 1.5–3×IQ), and asterisk represents extreme outliers (values >3×IQ).

As Table 3 shows, when only urban block metrics are considered, it is difficult to discriminate among both historical-town typologies (*historical1* and *historical2*), since few urban metrics enable to establish significant differences between them, i.e., mean built-up height, maximum built-up height, vegetation covered ratio, and normalized vegetation volume. As seen in Figure 7.a, buildings from *historical2* typology are lower than the ones from *historical1*, and also the coverage and volume of vegetation inside the urban-blocks are lower. One of the most noteworthy dissimilarities between both historical typologies is expressed by the street geometry descriptors, as evidenced the statistically significant differences showed by the metrics: mean street width, maximum street width, and minimum street width. Typically, *historical1* and *historical2* categories show narrower streets than the rest of urban typologies (Figure 8.a and Figure 8.b). There is also a clear difference in mean and median values of both historical-town typologies when taking into account the vegetation in the streets. Thus, *historical2* presents substantial lower values for UBRSA vegetation covered ratio metric, as Figure 8.c shows.

The mean and median values of the metrics characterizing the urban-block area and perimeter are significantly larger for *industrial* than for the rest of typologies (Figure7.d). Nevertheless, those geometry-related metrics show similar values for *r1950-60*, *r1970-80*, *r2000*, and *suburban*. Urban-block shape descriptors (compactness, shape index, and fractal dimension) do distinguish among those urban typologies, as seen in Table 3, although in this case the mean reached for *industrial* is not significantly different from that obtained in both historical typologies. In this case, the public street area surrounding each urban block ($Area_{UBRSA}$) enables to discriminate among *r1950-60, r1970-80*, and *r2000* urban typologies.

The metrics describing the height of the buildings show that lowest heights are given for *suburban* typology, followed by *industrial* and *historical2* (Figure 7.a). The high variability presented by *r2000* typology on the mean built-up height values is especially noticeable (Figure 7.b). Building coverage area values are strongly linked to the attributes characterizing the urban block dimensions, which determine the range of values that this metric can achieve. BCR avoids that limitation and it allows to discriminate among *r2000*, *suburban*, and *industrial*, and these from the rest of categories, since urban blocks containing these typologies are usually not completely occupied by constructions. This is particularly remarkable for *suburban* typology (Figure 7.e). Moreover, the ratio between the built-up coverage area and the UBRSA area promote the distinction among *rXIX*, *r1970-80*, and *r2000*. That metric values decrease for these typologies as more recent the constructions are (Figure 7.e and Figure 8.e).

The vegetation covered ratio inside urban blocks also significantly discriminates *suburban* among the other typologies (Figure7.c). This metric, however, is not as efficient in distinguishing the rest of classes, especially *historical1*, *rXIX*, and *r1970-80* (Table 3). If we consider the distribution of vegetation in the streets surrounding the urban blocks through the UBRSA vegetation covered ratio metric, it is noticeable that *r1950-60* lacks of green zones (Figure 8.c). Accounting the vegetation volume in the streets, the normalized UBRSA vegetation volume metric enables to discriminate *rXIX* from the rest of categories (Figure 8.d). This typology, given in consolidated areas, has a profuse abundance of voluminous vegetation in public spaces. Additionally, this metric permits to difference *r2000* from *rXIX*, *r1970-80*, and *suburban*, because vegetation in more recently built up neighbourhoods, though plentiful, is less voluminous. Complementing the above mentioned metrics we found that the ratio between the built-up coverage area within an urban block and the UBRSA area ($\text{Ratio}_{\text{Area}}$) enables to separate most recent constructions (*r2000* and *suburban*) from the oldest (*historical1* and *rXIX*) as is shown in Figure 8.d and Table 3. In turn, the ratio between the built-up volume and the UBRSA metric ($\text{Ratio}_{\text{Volume}}$) contribute to enhances the discrimination provided by the urban-block metrics: built-up volume and mean built-up volume (Figure 7.f), by boosting the differences concerning *rXIX* and *suburban*.

The results of applying the winnow algorithm show that the vegetation covered ratio is determined as the most relevant classification attribute when only considering urban block metrics, as shown in Table 5. This metric, as well as vegetation covered area, vegetation volume, and normalized vegetation volume, enables to easily distinguish *suburban* from other typologies (Figure 7.c). Furthermore, the vegetation covered ratio enables discriminate between *historical2* and *historical1*, and *historical1* with *r2000* and *suburban* (Table 3). This metric reaches the highest F-ratio value in the one-way ANOVA procedure among all analyzed metrics. The height of the buildings is also relevant being the mean built-up height ranked the 2nd, and the standard deviation of the buildings the 4th.

When urban-block and street metrics are combined the mean street-width value is ranked as the most significant attribute. These findings are in line with the reported by Loüw and Sithole (2011), who also stated the mean street-width as the most efficient attribute for classification. Although the metrics characterizing aspects of the streets different to the geometry – such as vegetation, or street geometry-buildings ratios – present a lower overall impact, they are still suitable for discriminating some particular urban typologies, as shown in Table 3.

The addition of metrics describing the streets to the classification process substantially increases the overall accuracy from 72.7% to 81.1%, which verifies that the combination of different types and contextual levels of characteristics provides a multidimensional description that significantly improves the characterization of urban structural typologies (Table 5). This outcome is consistent with the results reported by several authors (Wu et al., 2009; Gil et al., 2012; Hermosilla et al., 2012a).

Analyzing the particular user's and producer's accuracies reached by the urban typologies (Figure 9), *suburban* areas are better classified when only considering urban block metrics, reaching 91% and 98% for the user's and producer's accuracies, respectively. That is because this typology has a remarkably different appearance, featuring many vegetation and low buildings, and also the metrics describing those features are listed as the most significant for the classification (Table 4). The addition of the street metrics, however, has very limited effect on the accuracy of *suburban* typology. On the other hand, although *historical1* reaches fair user's and producer's accuracies, 76% and 80% respectively, with the urban block metrics. When the description of streets is included in the classification model, both indices have significantly increase up to 92%. The lowest accuracies are reached for *r1950-60* and *r1970-80*, which are transition typologies constructed between different eras. The addition of street metrics improves the discrimination of these typologies. This is in part accomplished due the contribution of the metrics: mean street width, vegetation covered ratio of UBRSA, and $\mathrm{Ratio}_{\mathrm{Area}}$, which cause notable accuracy increases for *r1950-60*, *r1970-80*, and also *r2000*. Additionally to these accuracy increments, the street metrics remarkably help to diminish the confusion between *r1950-60* and *r1970-80* with *historical1*, as well as *r1950-60* and *r2000* with *r1970-80*. Overall, *r1970-80* typology has the largest number of outliers in the metrics ranked as most significant in by winnow algorithm (see Figure 7 and Figure 8), which limits the positive effects of adding street metrics to eliminate the errors given between this class and *rXIX* and *r1950-60*, respectively.

5. Conclusions

This paper presents a set of urban metrics based on the description of the streets to quantify the various spatial patterns of the neighbourhoods constructed in different periods. These street metrics are proposed to complement the attributes derived from the urban blocks, providing a contextual frame to account the dissimilarities between the various construction typologies. We extract the urban metrics from high-spatial resolution multi-spectral images, airborne LiDAR data, and cadastral cartography containing the urban block boundaries. The performance of the street metrics is assessed for distinguishing among eight urban typologies within the metropolitan area of Valencia (Spain).

The results of the one-way ANOVA test show how the proposed street metrics help to establish statistically significant differences among some urban typologies where the urban block metrics present particular limitations. In addition, when analysing the importance of the urban metrics for the classification with the winnow algorithm, mean street width is revealed the most significant attribute, along with vegetation covered ratio per block and mean height of the buildings, and followed distantly by the building coverage ratio. Other street metrics characterizing aspects such as the distribution of vegetation in the street, or relationships between street geometry and buildings present a lower importance, but they are also appropriate for distinguishing among some urban typologies. The combination of the urban block attributes together with the street metrics causes an increase of the overall classification accuracy from 72.7% up to 81.1% with respects to use only urban block metrics. The addition of the street metrics positively affects to all the urban typologies, being the most benefited classes the main historical town, and residential areas constructed during 1950-1960 and 1970-1980.

This paper shows that use of metrics describing diverse properties of the streets provides a further description of the cities that complements the attributes extracted from the urban blocks. Thus, the outcomes of this study demonstrate the convenience of describing the street properties in order to provide useful urban metrics for all those applications requiring a precise characterization of the urban areas. This is important to note that the results achieved here show the local significance of the defined metrics for the specific case and urban typologies studied. Nevertheless, those descriptors may consistently be applied in diverse scenarios, the importance of these metrics varying to highlight the particular structural differences of the analysed cities.

Acknowledgements

The authors appreciate the financial support provided by the Spanish Ministry of Science and Innovation and FEDER in the framework of the project CGL2010-19591/BTE, and the material support of the Spanish *Instituto Geográfico Nacional* (IGN).

References

Anas, A., Arnott, R., & Small, K. A. (1998). Urban spatial structure. *Journal of economic literature, 36*(3), pp. 1426-1464.

Balsa-Barreiro, J., and Lois-González, R.C. (2009). Changes in the urban model of the city of Valencia (Spain): An analysis from the point of view of the published cartography. *In Urban Geography Commision, International Geographical Union (IGU/UGI): Emerging Urban Transformations, 2009 Meeting & International Conference on Multilayered Cities and Urban Systems* (30 July-10 August). CTOS, Osmana University, Hyderabad, India.

Bauer, T. and Steinnocher, K. (2001). Per-parcel land use classification in urban areas applying a rule-based technique. *GeoBIT/GIS, 6*, pp. 24-27.

Berger, C., Voltersen, M., Eckardt, R., Eberle, J., Heyer, T., Salepci, N., ... & Pacifici, F. (2013). Multi-Modal and Multi-Temporal Data Fusion: Outcome of the 2012 GRSS Data Fusion Contest. *IEEE journal of selected topics in applied earth observations and remote sensing*, *6*(3), pp. 1324-1340.

Boffet, A., and Serra, S. R. (2001). Identification of spatial structures within urban blocks for town characterization. *In Proceedings of 20th International Cartographic Conference,* pp. 1974-1983.

Bogaert, J., Rousseau, R., Hecke, P.V. & Impens, I. (2000). Alternative area-perimeter ratios for measurement of 2D shape compactness of habitats. *Applied Mathematics and Computation, 111* (1), pp. 71–85.

Canters F., Van de Voorde T., Batelaan O., Dams J., Cornet Y., Binard M., Goossens G., Devriendt D., Tack F., Engelen G., Lavalle C., Barredo J. (2007). Measuring and Modeling Urban Dynamics: Impact on Quality of Life and Hydrology. Objectives and Methodology, *In Proceedings of the IEEE International Geoscience and Remote Sensing Symposium* (IGARSS 2007), Barcelona, Spain, July 23-27, 2007, pp. 1994-1997.

Congalton, R., (1991). A review of assessing the accuracy of classifications of remotely sensed data. *Remote Sensing of Environment, 37*(1), pp. 35-46

Connors, J. P., Galletti, C. S., & Chow, W. T. (2013). Landscape configuration and urban heat island effects: assessing the relationship between landscape characteristics and land surface temperature in Phoenix, Arizona. *Landscape Ecology, 28*(2), pp. 271-283.

Douglas, D. H., & Peucker, T. K. (1973). Algorithms for the reduction of the number of points required to represent a digitized line or its caricature. *Cartographica: The International Journal for Geographic Information and Geovisualization, 10*(2), pp. 112-122.

Edussuriya, P., Chan, A., & Ye, A. (2011). Urban morphology and air quality in dense residential environments in Hong Kong. Part I: District-level analysis. *Atmospheric Environment, 45*(27), pp. 4789-4803.

Estornell, J., Ruiz, L. A., Velázquez-Martí, B., Hermosilla, T., (2012). Assessment of factors affecting shrub volume estimations using airborne discrete-return LiDAR data in Mediterranean areas. *Journal of Applied Remote Sensing, 6*, pp. 063544-1-063544-10.

Fowler, R. J., and Little, J. J. (1979). Automatic extraction of irregular network digital terrain models. In *ACM SIGGRAPH Computer Graphics, 13*(2), pp. 199-207.

Freund, Y., Schapire, R., & Abe, N. (1999). A short introduction to boosting. *Journal-Japanese Society For Artificial Intelligence, 14*(771-780), p. 1612.

Fukunaga, K., (1990). *Introduction to Statistical pattern recognition*. (2nd ed.), New York: Academic Press, ISBN: 978-0122698514, p. 592.

Furberg, D., and Ban, Y. (2008). Satellite monitoring of urban sprawl and assessing the impact of land cover changes in the Greater Toronto Area. *In The International Archives of The Photogrammetry, Remote Sensing and Spatial Information Sciences, ISPRS Congress*, Beijing. pp. 131-136.

Gamba, P., Dell'Acqua, F., & Dasarathy, B. V. (2005). Urban remote sensing using multiple data sets: Past, present, and future. *Information Fusion, 6*(4), pp. 319-326.

Gil, J., Beirão, J. N., Montenegro, N. & Duarte, J. (2009). On the discovery of urban typologies: data mining the many dimensions of urban form. *Urban Morphology, 16*(1), pp. 27-40.

Gong, C., Yu, S., Joesting, H., & Chen, J. (2013). Determining socioeconomic drivers of urban forest fragmentation with historical remote sensing images. *Landscape and Urban Planning, 117*, pp. 57-65.

González-Aguilera, D., Crespo-Matellan, E., Hernández-López, D., & Rodríguez-Gonzálvez, P. (2013). Automated Urban Analysis Based on LiDAR-Derived Building Models. *Geoscience and Remote Sensing, IEEE Transactions on, 51*(3), pp. 1844-1851.

Geiß, C., Taubenböck, H., Wurm, M., Esch, T., Nast, M., Schillings, C., & Blaschke, T. (2011). Remote sensing-based characterization of settlement structures for assessing local potential of district heat. *Remote Sensing, 3*(7), pp. 1447-1471.

Goodwin, N. R., Coops, N. C., Tooke, T. R., Christen, A., & Voogt, J. A. (2009). Characterizing urban surface cover and structure with airborne lidar technology. *Canadian Journal of Remote Sensing, 35*(3), pp. 297-309.

Heiden, U., Heldens, W., Roessner, S., Segl, K., Esch, T. & Mueller, A. (2012). Urban structure type characterization using hyperspectral remote sensing and height information. *Landscape and Urban Planning*, 105(4), pp. 361-375.

Hermosilla, T., Ruiz, L.A., Recio, J.A., Estornell J. (2011). Evaluation of Automatic Building Detection Approaches Combining High Resolution Images and LiDAR Data. *Remote Sensing 3*(6), pp. 1188-1210.

Hermosilla, T., Ruiz, L. A., Recio, J. A., & Cambra-López, M. (2012a). Assessing contextual descriptive features for plot-based classification of urban areas. *Landscape and Urban Planning, 106*(1), pp. 124-137.

Hermosilla, T., Gil-Yepes, J. L., Recio, J. A., & Ruiz, L. A. (2012b). Change Detection in Peri-urban Areas Based on Contextual Classification. *Photogrammetrie-Fernerkundung-Geoinformation*, *2012*(4), pp. 359-370.

Huck, A., S. Hese, & E. Banzhaf, (2011). Delineating parameters for object-based urban structure mapping in Santiago de Chile using QuickBird data. *The International Archives of the Photogrammetry, Remote Sensing and Spatial Information Sciences, 38* (4/W19), 6p.

Ji, W., Ma, J., Twibell, R. W., & Underhill, K. (2006). Characterizing urban sprawl using multi-stage remote sensing images and landscape metrics. *Computers, Environment and Urban Systems*, *30*(6), pp. 861-879.

Kellett, R., Christen, A., Coops, N. C., van der Laan, M., Crawford, B., Tooke, T. R., & Olchovski, I. (2013). A systems approach to carbon cycling and emissions modeling at an urban neighborhood scale. *Landscape and Urban Planning*, *110*, pp. 48-58.

Kressler, F. P., Bauer, T. B., & Steinnocher, K. T. (2001). Object-oriented per-parcel land use classification of very high resolution images. *In Remote Sensing and Data Fusion over Urban Areas, IEEE/ISPRS Joint Workshop 2001*, pp. 164-167.

Krummel, J.R., Gardner, R.H., Sugihara, G., O'Neill, V. & Coleman, P.R. (1987). Landscape patterns in a disturbed environment. *OIKOS*, *48*(3), pp. 321-324.

Laskari, S., Hanna, S., & Derix, C. (2008). Urban identity through quantifiable spatial attributes: Coherence and dispersion of local identity through the automated comparative analysis of building block plans. *In Proceedings of the third international conference on design computing and cognition*, Dordrecht, The Netherlands, pp. 615-634.

Lillebye, E. (1996). Architectural and functional relationships in street planning: an historical view. *Landscape and Urban Planning, 35*(2), pp. 85-105.

Littlestone, N. (1988). Learning quickly when irrelevant attributes abound: A new linear-threshold algorithm. *Machine learning*, 2(4), pp. 285-318.

Löuw, J., and Sithole, G. (2011). Context Based Detection of Urban Land Use Zones. Doctoral dissertation, University of Cape Town.

Lu, Z., Im, J., Quackenbush, L., & Halligan, K. (2010). Population estimation based on multi-sensor data fusion. *International Journal of Remote Sensing, 31*(21), pp. 5587-5604.

Malinverni, E. S. (2011). Change Detection Applying Landscape Metrics on High Remote Sensing Images. *Photogrammetric Engineering & Remote Sensing, 77*(10), pp. 1045-1056.

McGarigal, K. and Marks, B. J. (1995). Spatial pattern analysis program for quantifying landscape structure. *Gen. Tech. Rep. PNW-GTR-351. US Department of Agriculture, Forest Service, Pacific Northwest Research Station*.

Milliken, G.A. and Johnson, D.E. (1992). Analysis of messy data, Vol. 1, Designed experiments. Chapman & Hall/CRC. ISBN 10: 0412990814.

Murthy, S.K. (1998). Automatic construction of decision trees from data: A multi-disciplinary survey. *Data Mining and Knowledge Discovery, 2*(4), pp. 345-389.

Neidhart, H., and Sester, M. (2004). Identifying building types and building clusters using 3-D laser scanning and GIS-data. *In Geo-Imagery Bridging Continents, XXth ISPRS Congress*, Istanbul, pp. 715-720.

Novack, T., Kux, H. J. H., Feitosa, R. Q., & Costa, G. A. (2010). Per block urban land use interpretation using optical VHR data and the knowledge-based system Interimage. *The International Archives of the Photogrammetry, Remote Sensing and Spatial Information Sciences, 38*(4/C7), 6p.

Pan, X. Z., Zhao, Q. G., Chen, J., Liang, Y., & Sun, B. (2008). Analyzing the variation of building density using high spatial resolution satellite images: the example of Shanghai City. *Sensors, 8*(4), pp. 2541-2550.

Patino, J. E., and Duque, J. C. (2013). A review of regional science applications of satellite remote sensing in urban settings. *Computers, Environment and Urban Systems, 37*(1), pp. 1-17.

Peeters, A., & Etzion, Y. (2012). Automated recognition of urban objects for morphological urban analysis. *Computers, Environment and Urban Systems, 36*(6), pp. 573-582.

Puissant, A., Zhang, W. & Skupinski, G. (2012). Urban morphology analysis by high and very high spatial resolution remote sensing. *International Conference on Geographic Object-Based Image Analysis 4, (GEOBIA),* Rio de Janeiro, 7-9 May, pp. 524-529.

Quinlan, J.R., (1993). *C4.5. Programs for machine learning*. San Francisco. Morgan Kaufmann. ISBN: 1-55860-238-0, p. 302.

Robinson, D. (2006). Urban morphology and indicators of radiation availability. *Solar energy, 80*(12), pp. 1643-1648.

Taubenböck, H., Klotz, M., Wurm, M., Schmieder, J., Wagner, B., Wooster, M., & Dech, S. (2013). Delineation of Central Business Districts in mega city regions using remotely sensed data. *Remote Sensing of Environment, 136*, pp. 386-401.

Tompalski, P. and Wezyk, P. (2012). LIDAR and VHRS Data for Assessing Living Quality in Cities: An Approach Based on 3D Spatial Indices. *International Archives of Photogrammetry and Remote Sensing, (XXXIX-B6)*, pp. 173-176.

Tooke, T. R., vanderLaan, M., Coops, N., Christen, A., & Kellett, R. (2011). Classification of residential building architectural typologies using LiDAR. *In Proceedings of the Joint Urban Remote Sensing Event 2011* (11-13 April), Munich, Germany, pp. 221-224.

Tooke, T. R. and Coops, N. C. (2013). A Review of Remote Sensing for Urban Energy System Management and Planning. *In Proceedings of the Joint Urban Remote Sensing Event* 2013 (21-23 April). Sao Paulo, Brazil, pp. 167-170.

Vanderhaegen, S. and Canters, F. (2010). Using remote sensing data for improving the distinction between distinct types of urban land use and form using spatial metrics. *In Proceedings of the 30th EARSeL Symposium: Remote Sensing for Science, Education and Natural and Cultural Heritage*, Paris, 31 May- 3 June, European Association of Remote Sensing Laboratories, pp.757-764.

Van der Geer, J., Hanraads, J. A. J., & Lupton, R. A. (2010). The art of writing a scientific article. *Journal of Scientific Communications, 163*, pp. 51–59.

Wijnant, J. and Steenberghen, T. (2004). Per-parcel classification of urban ikonos imagery. *7th AGILE Conference on Geographic Information Science*, Heraklion, 29 April-1 May, pp. 447-455.

Wu, S.S., Qiu, X., Usery, E. L. & Wang, L. (2009). Using geometrical, textural, and contextual information of land parcels for classification of detailed urban land use. *Annals of the Association of American Geographers, 99*(1), pp. 76-98.

Yoshida, H., and Omae, M. (2005). An approach for analysis of urban morphology: methods to derive morphological properties of city blocks by using an urban landscape model and their interpretations. *Computers, environment and urban systems, 29*(2), pp. 223-247.

Yu, B., Liu, H., Wu, J., Hu, Y. & Zhang, L. (2010). Automated derivation of urban building density information using airborne LiDAR data and object-based method. *Landscape and Urban Planning, 98*(3-4), pp. 210-219.

Zhan, Q., Molenaar, M. & Gorte, B. (2000). Urban land use classes with fuzzy membership and classification based on integration of remote sensing and GIS. *The International Archives of Photogrammetry and Remote Sensing, 33*(B7/4; PART 7), pp. 1751-1759.

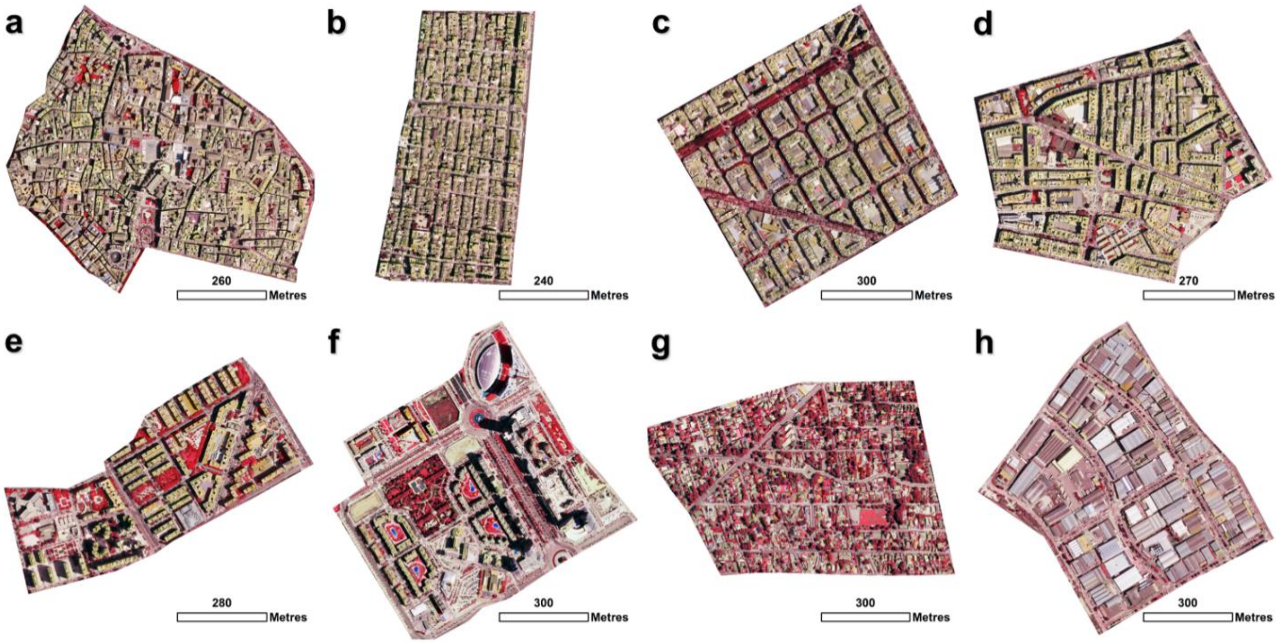

Figure 1. Examples of the urban typologies defined in a colour infrared composition: (a) Main historical town (*historical1*), (b) secondary historical town (*historical2*), (c) late XIX century expansion (*rXIX*), (d) 1950-1960s residential areas (*r1950-60*), (e) 1970-1980s residential areas (*r1970-80*), (f) 2000s residential areas (*r2000*), (g) single-family suburban housing areas (*suburban*), (h) industrial areas (*industrial*).

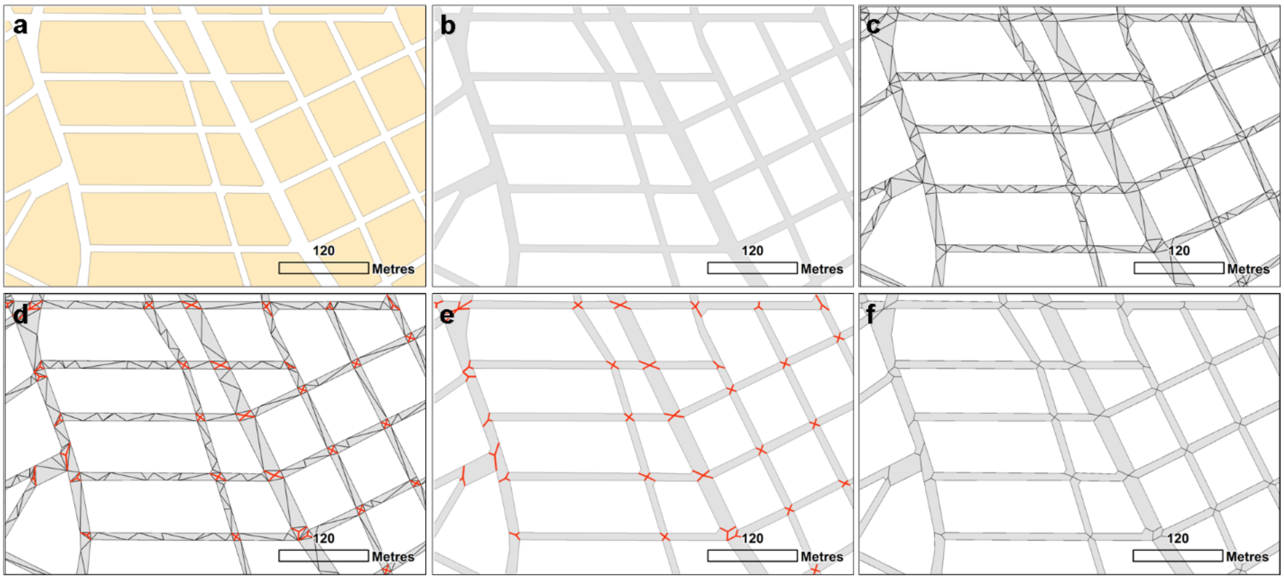

Figure 2. Steps followed to segment the public street: (a) simplified urban-blocks; (b) street polygon, computed as the complementary of the urban-blocks (in grey); (c) triangulated irregular network (TIN) of the street polygon; (d) identification of triangles within street crossings, computation of centroids, and delineation of street crossing boundaries (in red); (e) combination of neighbouring triangles; (f) resulting street segments.

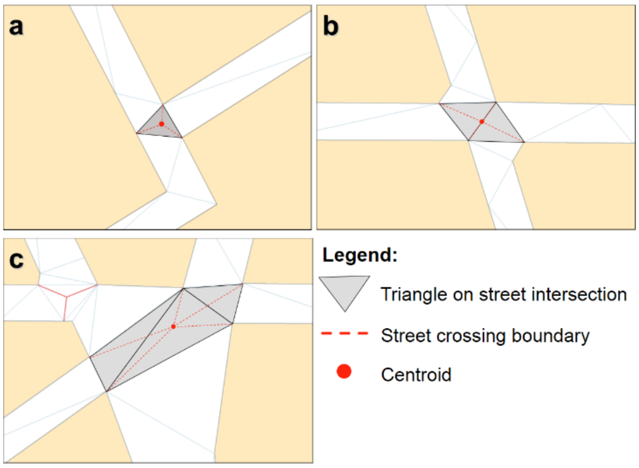

Figure 3. Definition of street crossing boundaries for street intersections composed by (a) one, (b) two, and (c) three triangles.

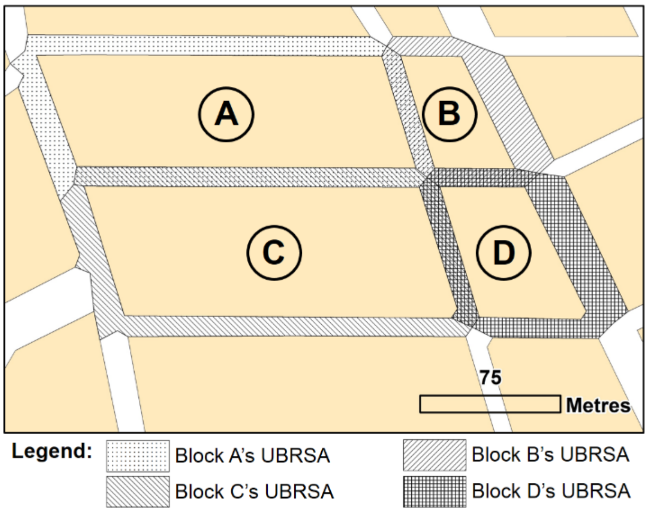

Figure 4. Example of overlapping urban-block related street area (UBRSA) polygons.

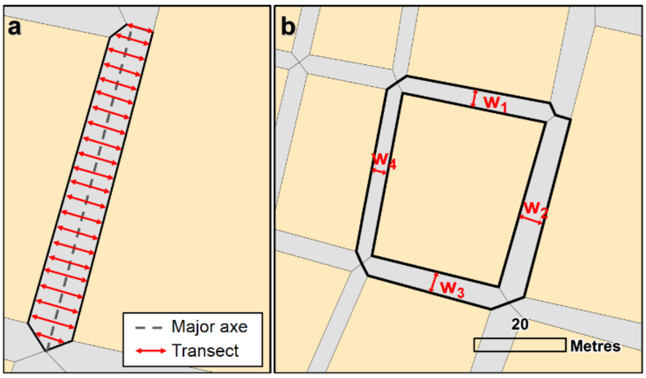

Figure 5. (a) Scheme of transects extracted to compute the median width value characterizing a street segment. (b) Street segments conforming a UBRSA used to derive street width metrics.

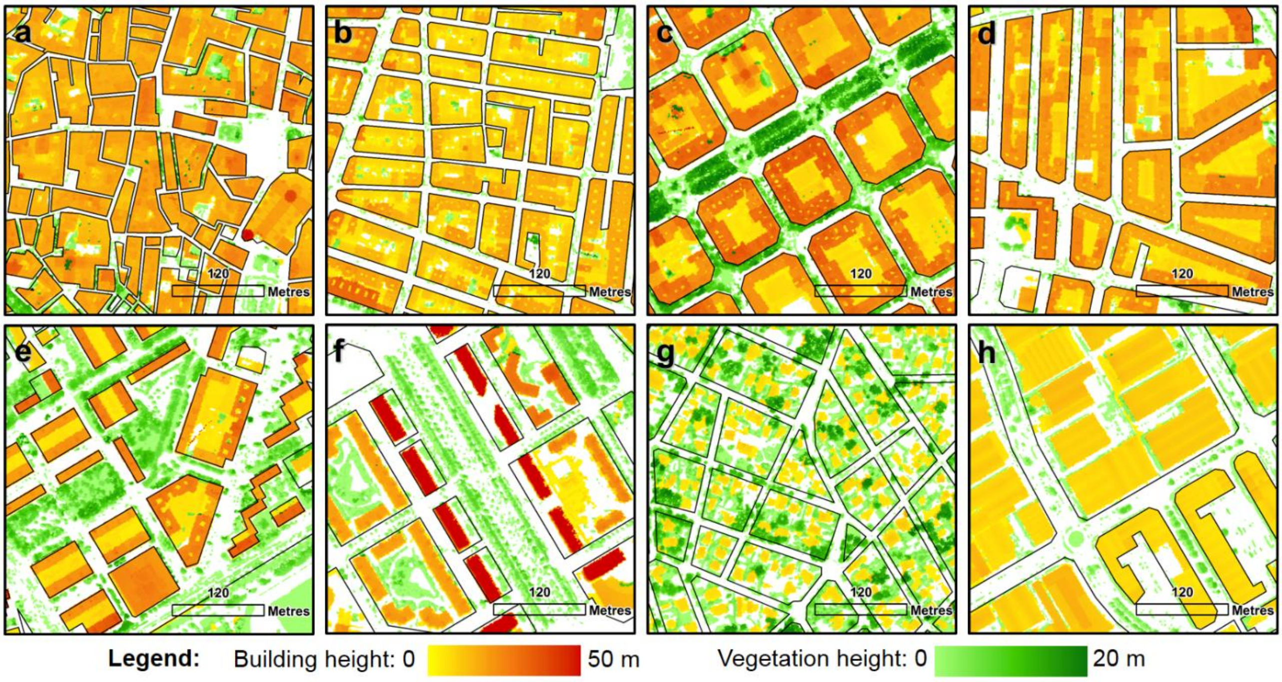

Figure 6. Details of buildings and vegetation height distribution for the urban typologies defined: (a) Main historical town (*historical1*), (b) secondary historical town (*historical2*), (c) late XIX century expansion (*rXIX*), (d) 1950-1960s residential areas (*r1950-60*), (e) 1970-1980s residential areas (*r1970-80*), (f) 2000s residential areas (*r2000*), (g) single-family suburban housing areas (*suburban*), (h) industrial areas (*industrial*).

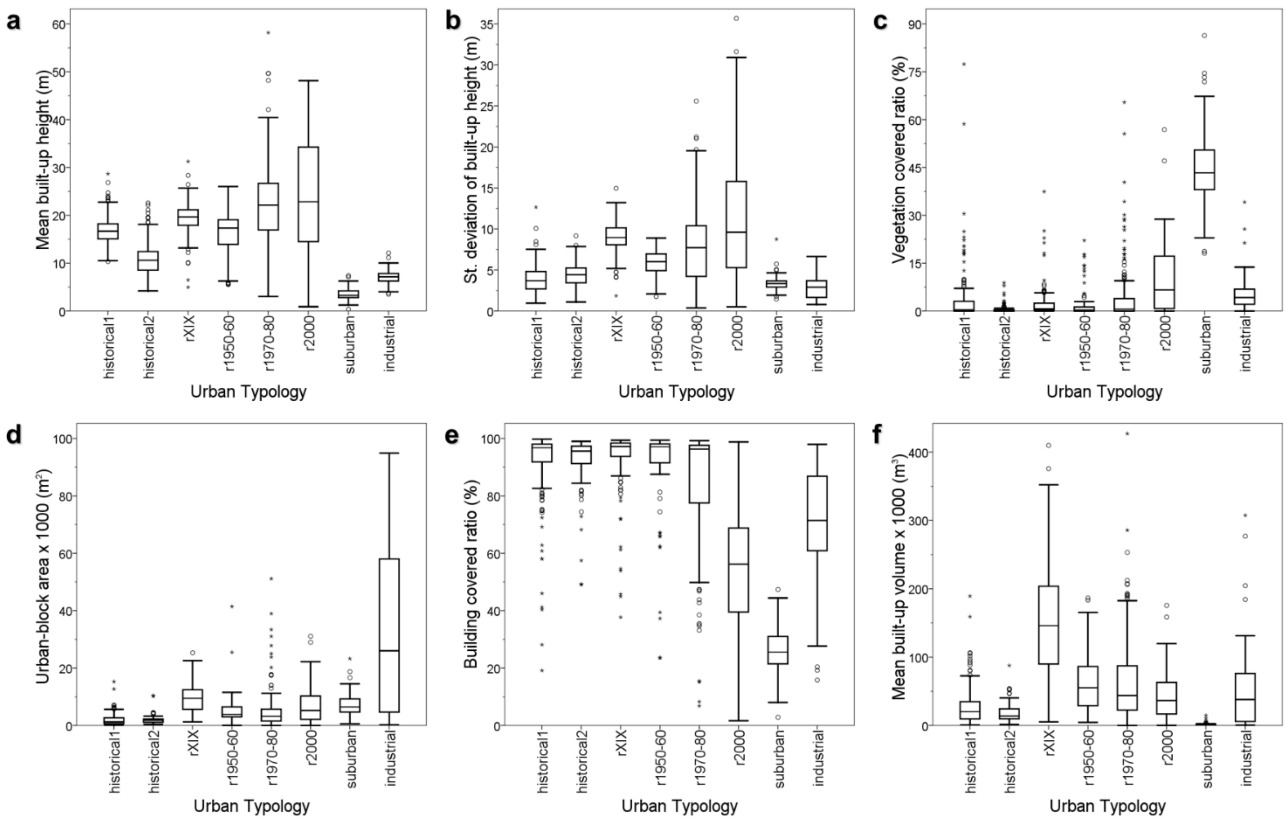

Figure 7. Relationship between urban typologies and urban-block metrics: (a) mean built-up height, (b) standard deviation of the built-up heights, (c) vegetation covered ratio, (d) urban-block area, (e) building covered ratio, and (f) mean built-up volume.

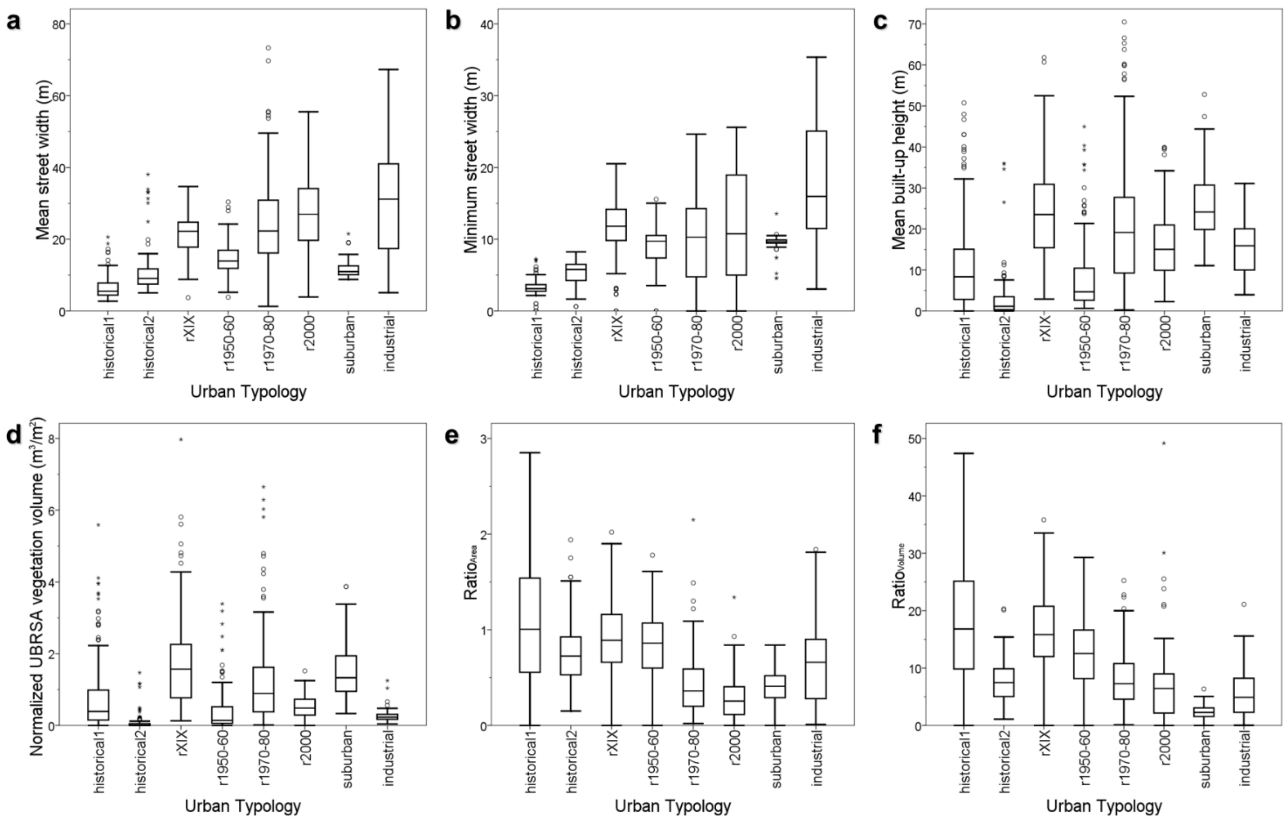

Figure 8. Relationship between urban typologies and street metrics: (a) mean street width, (b) minimum street width, (c) UBRSA vegetation covered ratio, (d) normalized UBRSA vegetation covered ratio, (e) ratio between built-up area within an urban block and UBRSA area, and (f) ratio between built-up volume and UBRSA area.

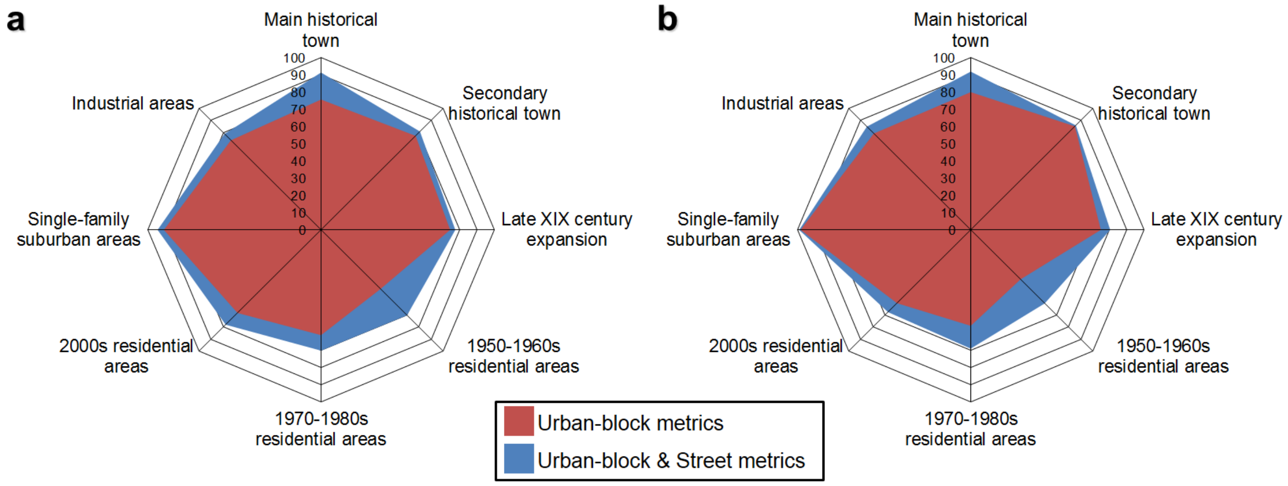

Figure 9. (a) User's and (b) producer's accuracies reached for each urban typology when considering only urban-block-based metrics or combining these with street-based metrics.

Table 1. Metrics and equations extracted from urban blocks.

Metric (units)	**Equation**
Area (m^2)	$Area_{UB}$
Perimeter (m)	$Perimeter_{UB}$
Compactness	$C = \frac{4 \cdot \pi \cdot Area_{UB}}{{Perimeter_{UB}}^2}$
Shape index	$SI = \frac{Perimeter_{UB}}{4 \cdot \sqrt{Area_{UB}}}$
Fractal dimension	$FD = 2 \cdot \frac{\log(Perimeter_{UB}/4)}{\log(Area_{UB})}$
Building coverage area (m^2)	$BCA = \sum_{i=1}^{b} r^2$
Building coverage ratio (%)	$BCR = \frac{BCA}{Area_{UB}} \cdot 100$
Mean built-up height (m)	$\overline{BH} = \frac{1}{b} \cdot \sum_{i=1}^{b} h_i$
Maximum built-up height (m)	$maxBH = \max\{h_i\}$
Standard deviation of building height (m)	$sdBH = \sqrt{\frac{1}{b-1} \cdot \sum_{i=1}^{b} (h_i - \overline{BH})^2}$
Number of buildings	N_B
Built-up volume (m^3)	$Volume_B = \sum_{i=1}^{b} h_i \cdot r^2$
Mean built-up volume (m^3)	$\overline{Volume_B} = \frac{Volume_B}{N_B}$
Normalized built-up volume (m^3/ m^2)	$nVolume_B = \frac{Volume_B}{Area_{UB}}$
Vegetation covered area (m^2)	$VCA = \sum_{i=1}^{v} r^2$
Vegetation covered ratio (%)	$VCR = \frac{VCA}{Area_{UB}} \cdot 100$
Vegetation volume (m^3)	$Volume_V = \sum_{i=1}^{v} h_i \cdot r^2$
Normalized vegetation volume (m^3/ m^2)	$nVolume_V = \frac{Volume_V}{Area_{UB}}$

b: total of pixels covered by buildings within the urba-block; *r*: spatial resolution; h_i: relative height obtained from the nDSM for the pixel *i*; *v*: total of pixels covered by vegetation.

Table 2. Metrics computed from the UBRSA.

Metric (units)	Formula
UBRSA area (m^2)	$Area_{UBRSA}$
Mean street width (m)	$\overline{SW} = \frac{1}{n} \cdot \sum_{i=1}^{n} w_i$
Standard deviation street width (m)	$sdSW = \sqrt{\frac{1}{n-1} \cdot \sum_{i=1}^{n} (w_i - \overline{SW})^2}$
Maximum street width (m)	$maxSW = \max\{w_i\}$
Minimum street width (m)	$minSW = \min\{w_i\}$
Number of neighbouring urban blocks	NN_{UB}
UBRSA vegetation covered area (m^2)	$VCA_{UBRSA} = \sum_{i=1}^{v} r^2$
UBRSA vegetation covered ratio (m^2)	$VCR_{UBRSA} = \frac{VCA_{UBRSA}}{Area_{UBRSA}} \cdot 100$
UBRSA vegetation volume (m^3)	$Volume_{VUBRSA} = \sum_{i=1}^{v} h_i \cdot r^2$
Normalized UBRSA vegetation volume (m^3/ m^2)	$nVolume_{VUBRSA} = \frac{V_{VUBRSA}}{Area_{UBRSA}}$
Ratio between the area of the buildings in a urban block and the area of the UBRSA	$Ratio_{Area} = \frac{BCA}{Area_{UBRSA}}$
Ratio between the built-up volume and the area of the UBRSA (m^3/ m^2)	$Ratio_{Volume} = \frac{Volume_B}{Area_{UBRSA}}$

n: number of adjacent street segments; w_i: street width of adjacent street segment *i*; *r*: spatial resolution; h_i: relative height obtained from the nDSM for the pixel *i*; *v*: number of pixels covered by vegetation within the UBRSA.

Table 3. Statistically significant different groups determined with Fisher's least significant difference procedure with a 95% of confidence level. Homogenous groups are identified using the same capital letter and sorted according their magnitude.

Metric	***historical1***	***historical2***	***rXIX***	***r1950 -60***	***r1970 -80***	***r2000***	***suburban***	***industrial***
$Area_{UB}$	A	A	C	B	B	BC	B	D
$Perimeter_{UB}$	A	A	C	B	B	B	B	D
Compactness	B	B	D	B	A	B	C	B
Shape index	B	B	A	B	C	C	A	B
Fractal Dim.	C	C	A	C	D	E	AB	BC
BCA	A	A	D	C	C	BC	AB	E
BCR	E	E	E	DE	D	B	A	C
$\overline{BH}$	D	C	E	D	F	G	A	B
$maxBH$	C	B	D	C	D	E	A	B
$sdBH$	AB	B	D	C	D	E	A	A
N_B	A	AB	AB	AB	BC	C	E	D
$Volume_B$	B	AB	D	C	C	C	A	E
$\overline{Volume_B}$	B	B	E	D	D	C	A	CD
$nVolume_B$	CD	BC	CD	BCD	D	E	A	AB
VCA	A	A	AB	AB	B	C	E	D
VCR	BC	A	B	AB	BC	D	E	C
$Volume_V$	AB	A	C	ABC	C	BC	D	C
$nVolume_V$	BCD	A	BCD	AB	D	CD	E	ABC
$Area_{UBRSA}$	A	A	C	B	C	D	B	E
$\overline{SW}$	A	B	D	C	E	E	B	F
$sdSW$	AB	BC	D	C	E	E	A	E
$maxSW$	A	BC	D	C	E	E	AB	E
$minSW$	A	B	F	C	DE	EF	CD	G
NN_{UB}	E	A	DE	CDE	BCD	BC	B	BCDE
VCA_{UBRSA}	A	A	C	AB	C	C	B	D
VCR_{UBRSA}	B	A	E	B	D	C	E	C
$Volume_{VUBRSA}$	A	A	C	AB	C	B	B	B
$nVolume_{VUBRSA}$	C	A	F	B	D	BC	E	AB
$Ratio_{Area}$	F	D	E	DE	B	A	AB	D
$Ratio_{Volume}$	F	C	E	D	C	BC	A	B

Table 4. Attributes selected by the winnow algorithm ranked by their classification significance considering only urban block metrics, or combining these with street metrics (identified with *)

Urban block metrics		**Urban block & Street metrics**	
Metric	**Significance**	**Metric**	**Significance**
VCR	33%	*$\overline{SW}$	44%
$\overline{BH}$	24%	VCR	42%
Compactness	10%	$\overline{BH}$	40%
sdBH	10%	BCR	9%
$Perimeter_{UB}$	8%	*$Ratio_{Area}$	5%
BCR	8%	*VCR_{UBRSA}	3%
$Area_{UB}$	4%	$Perimeter_{UB}$	1%
$Volume_{V}$	3%	$nVolume_{V}$	1%
Fractal dimension	2%	*maxSW	1%
maxBH	2%	*$nVolume_{VUBRSA}$	1%
BCA	1%	Fractal dimension	<1%
$Volume_{B}$	1%	$Volume_{B}$	<1%
N_{B}	1%	*NN_{UB}	<1%
$nVolume_{B}$	1%	*$Area_{UBRSA}$	<1%
Shape Index	<1%	*$Ratio_{Volume}$	<1%
VCA	<1%		
$nVolume_{V}$	<1%		

Table 5. Overall classification accuracy reached considering only urban block metrics or combining these with street metrics.

Urban metrics	**Overall accuracy**
Urban bock	72.7%
Urban block & Street	81.1%